

# Design and Simulation of $2 \times 2$ Micro Strip Circular Patch Antenna Array at 28 GHz for 5G Mobile Station Application

Salim Abdullah Hasan, Abdulsattar Mohamed Ahmed, Mohanad Nawfal Abdulqader,  
and Younis Shareef Dawood

**Abstract**—This paper proposes the design and simulation of  $2 \times 2$  circular patch antenna array working at 28 GHz by using four inset feed micro strip circular patch antennas to achieve beam forming with directivity around 13dB which is required to overcome part of high path loss challenge for high data rate mm-5G mobile station application. Four element  $2 \times 2$  array consists of two  $1 \times 2$  circular patch antenna arrays based on power divider and quarter wavelength transition lines as a matching circuit. The designed antenna array is simulated on RT/duroid 5880 dielectric substrate with properties of 0.5mm thickness, dielectric constant  $\epsilon_r=2.2$ , and tangent loss of 0.0009 by using Computer System Technology (CST) software. The performances in terms of return loss, 3D-radiation pattern is evaluated at 28 GHz frequency band. The design also includes the possibility of inserting four identical  $2 \times 2$  antenna arrays at four edges of mobile station substrate to achieve broad space coverage by steering the beams of the mobile station arrays.

**Keywords**—patch; 5G; return loss; dielectric; array; divider; substrate; directivity; bandwidth

## I. INTRODUCTION

THE recent years, a huge number of smart devices and sensors providing big amount of information is increasing rapidly due to the presence of several Information Technology fields (IT) such as Artificial Intelligence (AI), and Internet of Thing (IoT). Beside this the number of smart phones, tablets, etc is increasing also to support existing services as internet, music, gaming with high quality. This tends to huge data content hence high data rate information ( $> 10\text{Gbit/s}$ ) is required which do not match as well today's access wireless mobile networks (3G,4G mobile system).

The new generation 10 Gbit/s-mm-5G mobile communication system is proposed to support such high data services. To transfer such high data rate through 5G system the RF frequency band must be higher at least three times than the data rate, therefore the RF frequency band

will be around 30 GHz. Accordingly on July 2016 the Federal Communication Commission (FCC) voted to adopt for 5G project a new mm-Wave licensed frequency bands namely 28-GHz frequency band (27.5–28.35GHz), 38-frequency band (37–38.6 GHz), and 39-frequency band (38.6–40 GHz) [3]. These frequency bands lead to high path loss challenge. To overcome such high path loss, a high antenna gain is required at the base station and mobile phone, therefore a high gain rectangular planer arrays antenna system must be investigated. As in [4] the link budget calculation show that the antenna gain required for 5G-mobile phone must be  $\geq 13\text{dB}$  and at base station must be  $\geq 25\text{ dB}$  to compensate high path loss and achieve transmission distance less or equal 250m.

To cover above antenna gain requirement, this research work propose a design and simulation of four element  $2 \times 2$  micro strip circular patch planner antenna array based on power divider and quarter wavelength impedance transformer characteristic to achieve beam forming with directivity around 13 dB.

The single micro strip circular patch antenna shown in Fig. 1 is proposed in this design as a basic element of  $2 \times 2$  array because it has low profile and easy to be fabricated on dielectric substrate and integrated with electronic components of the mobile phone. The proposed micro strip circular patch consists of circular conducting patch with thickness  $t \ll \lambda$  is placed on one side of dielectric substrate with thickness  $h$  within the range ( $0.003\lambda \leq h \leq 0.05\lambda$ ) while the ground placed on the other side of the substrate with thickness  $t \ll \lambda$  where  $\lambda$  is the operating wavelength. There are various substrates that can be used for the design of micro strip patch antenna and their dielectric constants are usually in the range  $2 \leq \epsilon_r \leq 12$ [9]

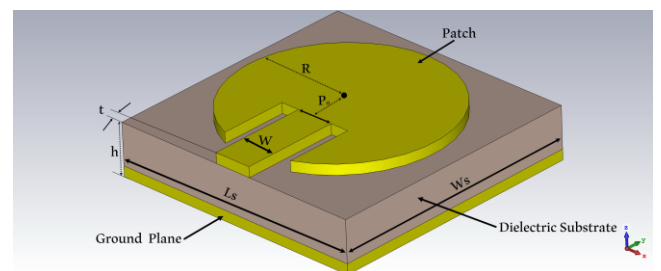


Fig. 1. 3D Conventional inset feed circular patch antenna structure

This work was supported by GigaNet ISP Company.

Authors are with Computer Technical Engineering Department at Al-Hadbaa University College, Mosul, Iraq (e-mail: salimhasan1954@gmail.com, abdulsattar54@yahoo.com, mohanad.alhyaly@gmail.com, younisalshareef@gmail.com).



The proposed  $2 \times 2$  antenna array is composed of two  $1 \times 2$  circular patch antenna arrays each consists of two single inset feed micro strip circular patch antenna, (50-100 $\Omega$ ) power divider to divide the power between the elements of the array equally, and two 70.7 quarter wavelength transition lines to match two 100  $\Omega$  output port feed lines of divider with 50 $\Omega$  inset feed lines of the patches.

To form four element  $2 \times 2$  patch antenna array a (25-50 $\Omega$ ) three port power divider is used to divide the power between the two  $1 \times 2$  arrays equally, and 35.35 $\Omega$  quarter wavelength transition line to match 50 $\Omega$  input feed line to 25 $\Omega$  pinport feed line of the power divider.

The (RT/duroid 5880) dielectric is proposed as substrate material with thickness 0.5 mm in this design since it has a low dielectric constant  $\epsilon_r = 2.2$  in order to achieve a maximum antenna directivity as possible at 28 GHz frequency range.

## II. SINGLE PATCH ANTENNA DESIGN

The top view of single inset feed circular patch antenna shown in Fig. 1 are sketched as in Fig. 2. The patch and ground planes for the proposed antennas are assumed to be printed on the (RT/duroid 5880) dielectric substrate which has low dielectric constant  $\epsilon_r = 2.2$  in order to achieve a maximum antenna directivity as possible. The dimensions of antenna structural parameters such as patch radius  $a$ , feeding point location  $P_o$ , the width  $w$  and length  $L_f$  of inset feed micro strip transmission line shown in Fig. 2 should be calculated. To achieve the calculation of the previous patch dimensions three important parameters must be available are (the frequency of operation  $f$ , the dielectric constant of the substrate  $\epsilon_r$  and the thickness of the dielectric substrate  $h$ ) as in the following subsections.

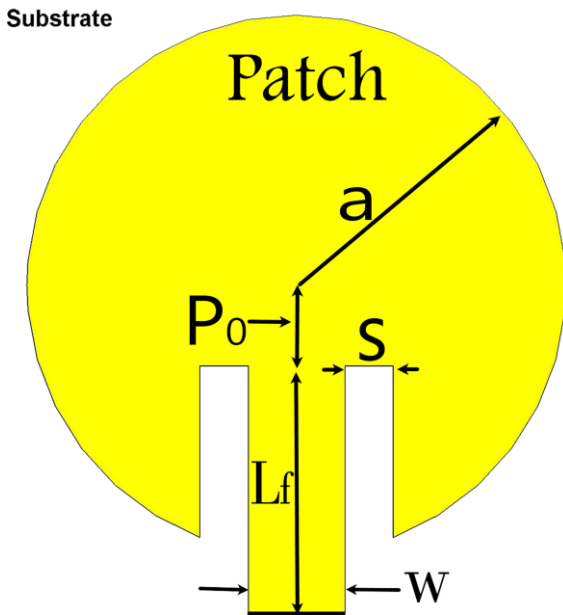


Fig. 2. Top view of the proposed inset feed circular micro strip patch antenna

### A. Substrate thickness selection

The thickness  $h$  of the substrate must be within the design condition  $(0.003\lambda \leq h \leq 0.05\lambda)$ [9], therefore for  $\lambda=10.7$  mm at  $f=28$  GHz, then the required thickness must be within  $0.00321 \leq h \leq 0.535$ mm. In this work the thickness  $h=0.5$  mm has been taken.

### B. Actual and effective radius calculation

The actual radius of the patch  $a$  is given by the following approximate expression [9].

$$a = \frac{F}{\left\{1 + \frac{2h}{\pi \epsilon_r F} \left[ \ln \left( \frac{\pi F}{2h} \right) + 1.77726 \right] \right\}^{\frac{1}{2}}} \quad (1)$$

Were

$$F = \frac{8.791 \times 10^9}{f \sqrt{\epsilon_r}}$$

To take into consideration, the fringing effect, then the effective radius  $a_e$  of patch is used and is given by [9].

$$a_e = a \left\{ 1 + \frac{2h}{\pi \epsilon_r a} \left[ \ln \left( \frac{\pi a}{2h} \right) + 1.77726 \right] \right\}^{\frac{1}{2}} \quad (2)$$

### C. The dimensions of inset micro strip feed line calculation

The characteristic impedance of micro strip line is given by the following equation [9]

$$Z_o = \begin{cases} \frac{120\pi}{\sqrt{\epsilon_{\text{reff}}} \left[ \frac{w}{h} + 1.393 + 0.667 \ln \left( \frac{w}{h} + 1.444 \right) \right]} & \text{for } \frac{w}{h} > 1 \\ \frac{60}{\sqrt{\epsilon_{\text{reff}}}} \ln \left( \frac{8h}{w} + \frac{w}{4h} \right) & \text{for } \frac{w}{h} < 1 \end{cases} \quad (3)$$

Using (3) the width of inset micro strip feed line shown in Fig. 2 can be calculated

The length  $L_f$  of inset feed line shown in Fig 2 can be calculated by [18],

$$L_f = \frac{c}{4f\sqrt{\epsilon_r}} \quad (4)$$

### D. Inset cut of the inset feed line micro strip line calculation

Resonant frequency of patch antenna depends on inset cut (S). Expression which relates inset cut and resonant frequency can be calculated by [19]

$$S = \frac{c}{\sqrt{2\epsilon_{\text{reff}}}} \frac{4.65 \times 10^{-12}}{f_{\text{GHz}}} \quad (5)$$

Where  $C = 3 \times 10^8$ m/s

### E. Inset feeding point location calculation

In this design inset feed line has been used as shown in Fig. 2. The feeding point must be located at  $\rho = P_o < a_e$  from the center of the circular patch so that the edge input resistance at  $\rho = a_e$  of circular patch will reduce to a value that must match the characteristic impedance  $Z_o = 50 \Omega$  of the inset feed micro strip line. The input resistance of

circular patch with inset feed at any radial distance  $\rho = P_o$  from the centre of the patch is given by [9]

$$R_{in}(\rho' = P_o) = R_{in}(\rho' = a_e) \frac{j_1^2(kP_o)}{j_1^2(ka_e)} \quad (6)$$

Where  $R_{in}(\rho = a_e)$  is the edge input resistance of the patch given by [9]

$$R_{in}(\rho' = a_e) = \left[ \frac{(ka_e)^2}{480} \int_0^{\frac{\pi}{2}} [j'_{02} + \cos^2\theta j'_{22}] \sin\theta d\theta \right]^{-1} \quad (7)$$

$a_e$  is the effective radius given by (2)

$$j_{02} = j_0(ka_e \sin\theta) + j_2(ka_e \sin\theta) \quad (8)$$

$$j'_{02} = j_0(ka_e \sin\theta) - j_2(ka_e \sin\theta) \quad (9)$$

and  $k$  is the phase constant given by

$$k = \frac{2\pi}{\lambda} = \frac{2\pi f}{c} \quad (10)$$

#### F. Calculated results of the designed patch dimensions

With the help of previous formulae mentioned in subsections B to E the calculated of circular patch dimensions are summarized as in table I.

TABLE I  
CALCULATED RESULTS OF THE DESIGNED PATCH DIMENSION

Parameter		Calculated result
Actual radius	$a$	1.893 mm
Substrate thickness	$h$	0.5 mm
Effective radius	$a_e$	2.135 mm
Feed line width		1.554 mm
$w_{50}$		
Feed line length	$L_f$	1.8
Feeding location	$P_o$	0.6 073 mm
Inset feed cut	$S$	0.29 mm

#### G. Simulation results of single circular patch antenna

The CST program has been used to simulate the proposed single inset feed circular micro strip patch antenna working at frequency  $f=28$  GHz. The calculated dimensions of patch antenna shown in table 1 are used in the simulation. After simulation the optimized dimensions of the designed single circular patch antenna are summarized as in table. II.

TABLE II  
OPTIMIZED DIMENSIONS OF THE DESIGNED SINGLE PATCH

Parameter		Optimized dimensions
Actual Radius	$a$	2.32
(mm)		
Substrate thickness	$h$	0.37
(mm)		
Inset line feed width		1.15
$w_{50}$ (mm)		
Feeding location	$P_o$	0.653
(mm)		
Inset feed line length		2.33
$L_f$ (mm)		
Inset feed cut	$S$ (mm)	0.575

The simulation result of return loss  $S_{11}$  is shown as in Fig. 3. It could be seen that the patch antenna resonates at 28.018 GHz with return loss  $S_{11} \cong -39$  dB.

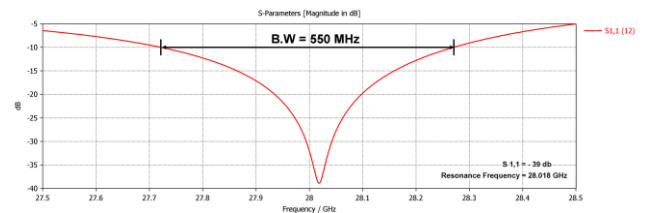


Fig. 3. Return loss  $S_{11}$  for single circular patch antenna

Fig. 4 shows the simulation results of 2D and 3D radiation patterns for single circular patch antenna, where it could be seen that the 3D directivity is  $D_o = 7.68$  dB, H - plane HPBW is  $\theta_H = 81^\circ$ , and E-plane HPBW is  $\theta_E = 72^\circ$ .

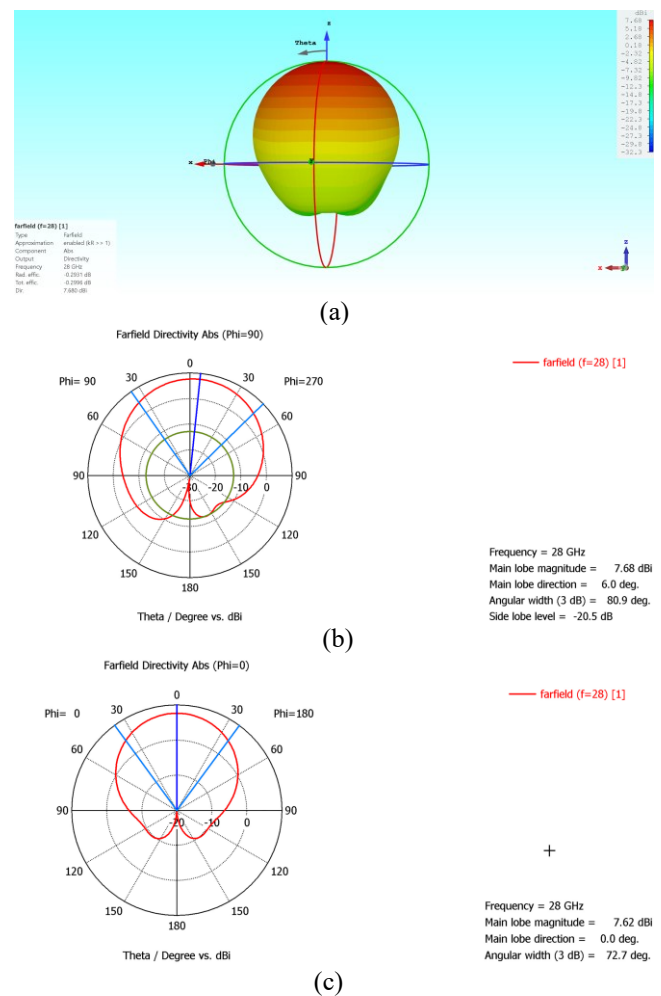


Fig. 4. Simulation results of radiation patterns for single patch antenna (a) 3D gain (b) 2D in H-plane (c) 2D in E-plane

### III. TWO ELEMENT 1 x 2 CIRCULAR PATCH ANTENNA ARRAY DESIGN

The geometry of 1x2 circular patch antenna array is shown in Fig. 5. This geometry consists of two previous designed low profile inset feed circular patch antennas each of them has the same optimized dimensions shown in table. II, three

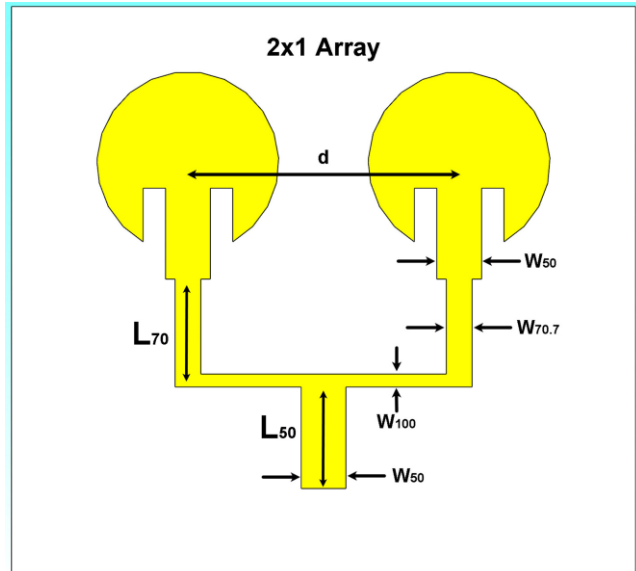


Fig. 5. Geometry of  $1 \times 2$  micro strip circular patch antenna array.

ports ( $50\text{--}100\Omega$ ) power divider to divide the power between the patches equally and two transition micro strip feed lines having length equal quarter of operating wavelength ( $\lambda/4$ ) are used to match two  $100\Omega$  output ports micro strip feed lines of the divider to two  $50\Omega$  inset feed micro strip lines of the circular patches. The impedance  $Z_q$  of the quarter wave transition line can be calculated by using

$$Z_q = \sqrt{Z_L Z_C} \quad (11)$$

Where,  $Z_L = 50\Omega$  is the impedance of inset feed line and  $Z_C = 100\Omega$  is the impedance of output port feed lines of the power divider. For the previous values of  $Z_L, Z_C$  and using (11) we get  $Z_q = 70.7\Omega$ .

#### A. Design of 3-port (50-100Ω) power divider

We assume that length of input port feed line  $L_{50} = 0.25\lambda$ , length of each transition line  $w_{70.7} = 0.25\lambda$ , and length of each output port fed line  $L_{100} = dy = 0.5\lambda$ . The dimensions of the divider are calculated by using (3) for optimum substrate thickness  $h=0.37\text{mm}$  and dielectric constant  $\epsilon_r=2.2$  and summarized as in table III.

TABLE III  
CALCULATED DIMENSION OF 3-PORT (50-100Ω) POWER DIVIDER

Parameter	Calculated result
50Ω input port feed line width $w_{50}$ (mm)	1.15
100Ω output port feed line width $w_{100}$ (mm)	0.3326
70.7Ω transition line width $w_{70.7}$ (mm)	0.6597

#### B. Simulation of $1 \times 2$ circular patch antenna array

The CST-software has been used to simulate the two element array structure shown in Fig. 5 by making use of the same optimized dimensions of single patch shown in

Table II, and the calculated dimensions of 3-port( $50\text{--}100\Omega$ ) power divider shown in table.3. The simulation results for 3-port( $50\text{--}100\Omega$ ) power divider dimension are shown in table IV.

TABLE IV  
OPTIMIZED DIMENSIONS OF 3-PORT (50-100Ω) POWER DIVIDER

Parameter	Optimized dimensions(mm)
50Ω line width $w_{50}$	1.15
50Ω line length $l_{50}$	$2.6 < 0.25\lambda$
Element spacing $dy$	$0.6128\lambda$
100Ω lines length $l_{100}$	$0.6128\lambda$
100Ω lines width $w_{100}$	0.3326
70.7Ω line width $w_{70.7}$	0.6597
70.7Ω line length $l_{70.7}$	$2.42857 < 0.25\lambda$

The simulation performance result of return loss  $S_{11}$  is shown in Fig. 6 for particular element spacing's ( $0.5\lambda, 0.55\lambda, 0.6128\lambda, 0.625\lambda, 0.65\lambda$ )

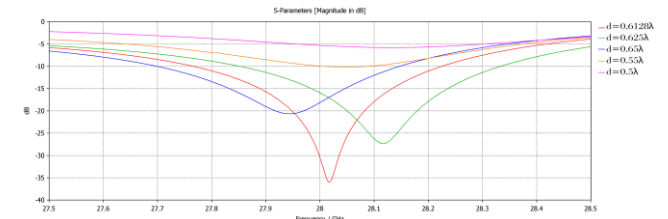


Fig. 6. Comparison of Return loss  $S_{11}$  for  $1 \times 2$  circular patch antenna array with particular element spacing's ( $0.5\lambda, 0.55\lambda, 0.6\lambda, 0.625\lambda, 0.65\lambda$ )

The performance simulation results of  $1 \times 2$  patch antenna array for different particular inter element spacings are summarized as in Table V.

TABLE V  
PERFORMANCE SIMULATION RESULTS OF  $1 \times 2$  CIRCULAR PATCH ANTENNA ARRAY FOR DIFFERENT ELEMENT SPACINGS

Spacing $dy$	$0.5\lambda$	$0.55\lambda$	$0.6128\lambda$	$0.625\lambda$	$0.65\lambda$
$f_r$ GHz	28.133	28.05	28.018	28.116	27.9
$S_{11}$ dB	-5.8	-10.21	<b>-35.6</b>	-27.5	-20.6
3Ddirectivity(dB)	10.4	10.5	10.6	10.7	10.8
BW (MHz)	-----	80	457	479	444
E-Plane HPBW $\theta_E$	$47^\circ$	$44^\circ$	$36.2^\circ$	$35.2^\circ$	$35^\circ$
H-Plane HPBW $\theta_H$	$80^\circ$	$79^\circ$	$78.4^\circ$	$77.8^\circ$	$76.5^\circ$
Normalized side lobe magnitude dB in E-plane		-20	-15.1	-13.43	-12.1

It could be seen from table. 5 that the optimum element spacing is at  $dy = 0.6128\lambda$  because the return loss  $S_{11}$  has minimum value at this spacing. As the element spacing increased the 3D-directivity, and the impedance bandwidth are slightly increased, HPBW in E-plane is decreased (beam forming) while the HPBW in H-plane remain almost the same values(no-beam forming). Also the normalized side lobe magnitude grows as the element spacing increased and this will lead to performance degradation in the the presence of electromagnetic interference.

Figure 7 shows the simulation results of 3D and 2D radiation patterns of  $1 \times 2$  circular patch antenna array for optimum element spacing  $dy = 0.6128\lambda$

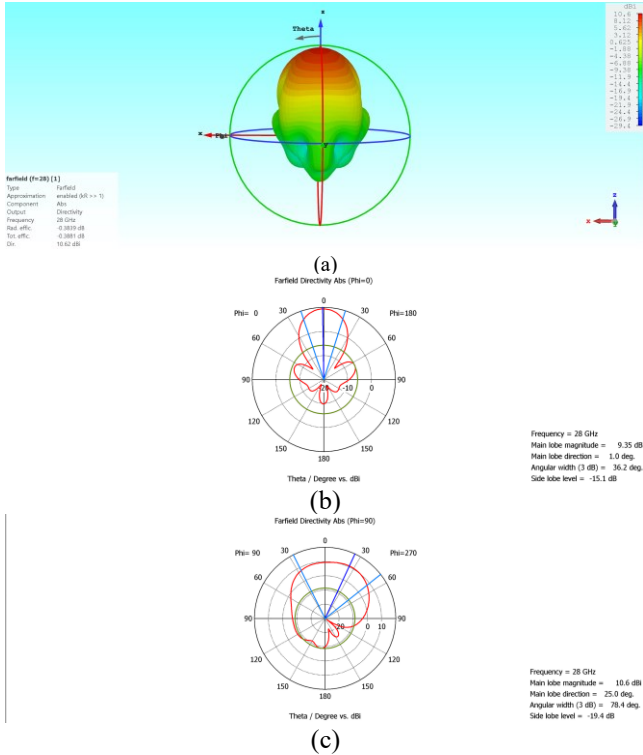


Fig.7. Simulated radiation patterns at 28 GHz of  $1 \times 2$  circular patch antenna array for optimum element spacing  $0.6128 \lambda$  (a) 3D (b) 2D in E-plane (c) 2D in H-plane.

#### IV. FOUR ELEMENT $2 \times 2$ CIRCULAR PATCH ANTENNA ARRAY DESIGN

The geometry of  $2 \times 2$  circular patch antenna array is shown in the Fig. 8. This geometry consists of two identical previous designed  $1 \times 2$  two element circular patch antenna array, 3-ports ( $25-50\Omega$ ) power divider to divide the power between the  $1 \times 2$  arrays equally and transition micro strip feed line having length equal quarter of operating wavelength ( $\lambda/4$ ) is used to match  $50\Omega$  input main feed line to  $25\Omega$  input port feed line of the power divider.

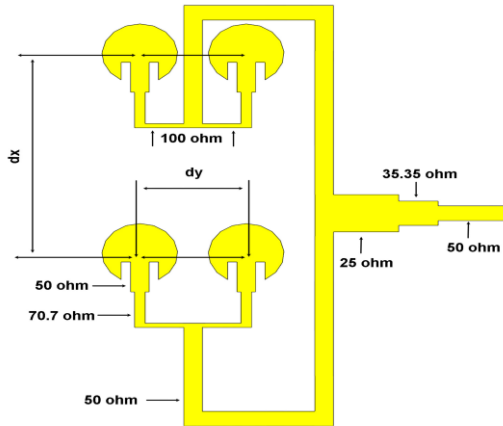


Fig. 8. Geometry of  $2 \times 2$  circular patch antenna array

The impedance  $Z_q$  of the quarter wave transition line can be calculated by using (11). Therefore for the impedance of

main input feed line  $Z_c = 50\Omega$ , and the impedance of input port feed line of the power divider  $Z_L = 25\Omega$  we get  $Z_q = 35.35 \Omega$ .

#### A. Design of 3-port 25-50Ω power divider

The dimensions of the divider are calculated by using (3) for optimum substrate thickness  $h = 0.37\text{mm}$  and dielectric constant  $\epsilon_r = 2.2$  and summarized as in Table 6.

TABLE VI  
CALCULATED DIMENSIONS OF ( $25-50\Omega$ ) 3-PORT POWER DIVIDER

Parameter	Calculated dimension (mm)
$50 \Omega$ input feed line width $w_{50}$	1.15
$25 \Omega$ input port feed lines width $w_{25}$	2.9
$50 \Omega$ output port feed lines width $w_{50}$	1.15
$35.35\Omega$ transition line width $w_{35.35}$	1.866
$35.35\Omega$ transition line length $L_{35.35}$	$0.25\lambda$

#### B. Element spacing calculation for $2 \times 2$ antenna array

The optimized spacing in y-direction  $dy = 0.6128\lambda$  is determined previously as shown in table. 5. It could be seen from the structure of  $2 \times 2$  circular patch antenna array shown in Fig. 8 that the minimum spacing in x-direction  $dx$  must be calculated by using the following inequality in order to avoid the over lapping between the two  $1 \times 2$  circular patch antenna arrays,

$$d_x > a + L_f + w_{100} + P_o + L_{70.7} \quad (12)$$

Substitution into above inequality from table 2 for the optimized values of  $a = 2.32 \text{ mm}$ ,  $L_f = 2.33$ ,  $P_o = 0.65 \text{ mm}$ , and from table 4 for the optimized values of  $L_{70.7} = 2.42857 \text{ mm}$   $w_{100} = 0.3326 \text{ mm}$  we get,

$$d_x > 8 \text{ mm or } d_x > 0.75 \lambda \quad (13)$$

In this design according to inequality given by (13) the optimum element spacing in x-direction has been selected as  $0.85\lambda$  in order to keep minimum side lobe magnitude as possible.

#### C. Simulation of $2 \times 2$ patch antenna array

The structure of  $2 \times 2$  patch antenna array shown in Fig. 8 has been simulated by making use of the previous optimized dimensions of  $1 \times 2$  antenna array shown in Table IV, and the calculated dimensions of ( $25-50\Omega$ ) power divider shown in table 6 as well as the previous selected element spacing  $dx = 0.85 \lambda$ . The simulation results are shown as in Fig. 9.

It could be seen from the simulation results shown in Fig. 9(a) that the  $2 \times 2$  array achieve return loss  $S_{11} = -32\text{dB}$  at resonance frequency  $f_r = 27.979 \text{ GHz}$ ,  $700\text{MHz}$  impedance bandwidth and from Fig. 19(b) the 3D directivity is  $Do = 12.7 \text{ dB}$ , the optimum value of HPBW in H - plane  $\theta_H = 45^\circ$  while in E-plane HPBW  $\theta_E = 36.2^\circ$  as shown in Table V.

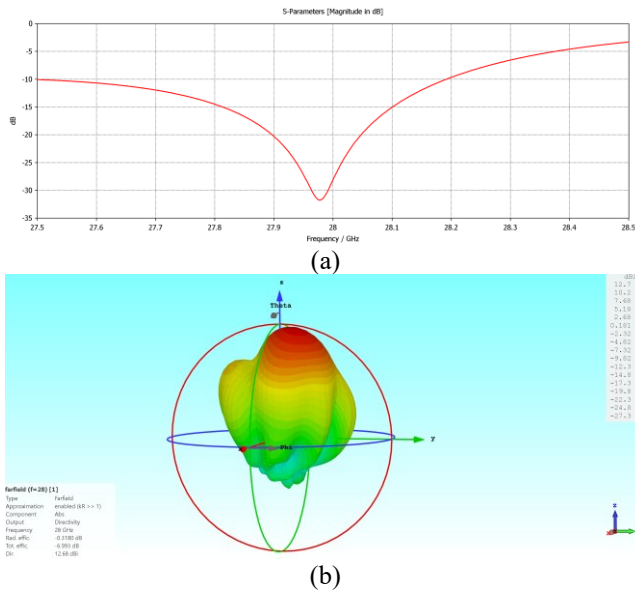


Fig. 9. Simulation results for  $2 \times 2$  circular patch antenna array with optimum element spacing  $dy = 0.6128\lambda$  and spacing  $dx = 0.85\lambda$ , (a) return loss  $S_{11}$  (b) 3D-radiation pattern

D. Comparison of simulation results

Comparison of 3D-radiation patterns for single micro strip circular patch antenna, two element  $1 \times 2$  antenna array, four elements  $2 \times 2$  antenna array is shown as in Fig. 10. It could be seen from Fig. 10 that the beam forming has been achieved as the number of patch elements increased. Also, Comparison of performance simulation results are summarized as in table 7. It could be seen from table 7 that as the number of patch elements increased the following are achieved

1. The HPBW in E & H-planes are decreased (beam forming)
2. The return loss  $S_{11}$ , 3D-gain, are increased.

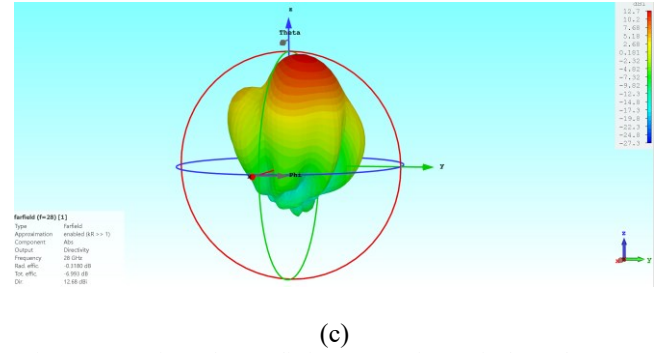


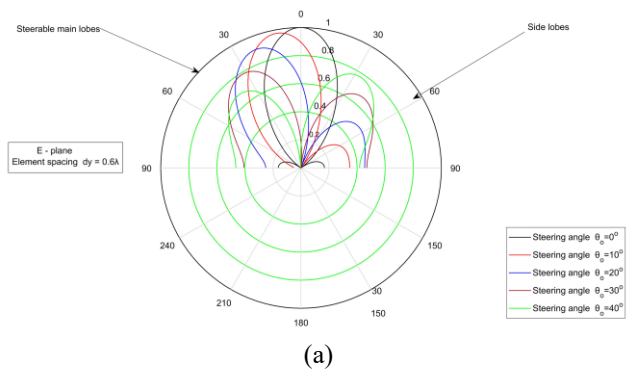
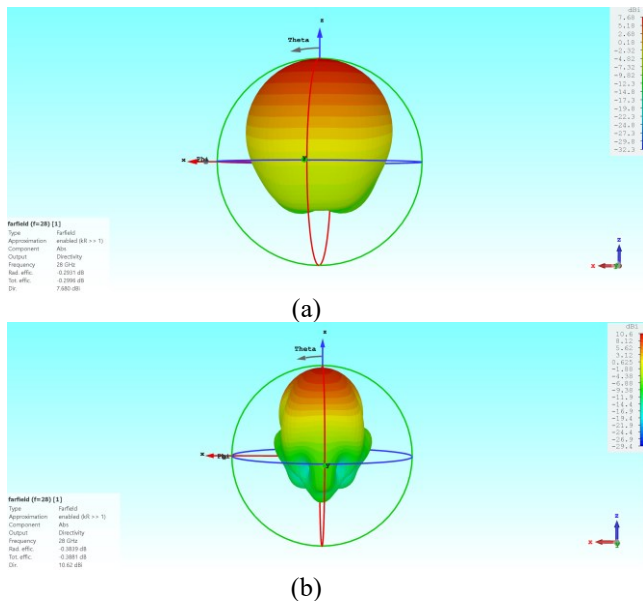
Fig. 10. comparison of 3D-radiation patterns for (a) single patch antenna (b)  $1 \times 2$  patch antenna array (c)  $2 \times 2$  patch antenna array

TABLE VII  
COMPARISON OF SIMULATION RESULTS FOR THE DESIGNED SINGLE PATCH ANTENNA,  $1 \times 2$  CIRCULAR PATCH ANTENNA ARRAY,  $2 \times 2$  CIRCULAR PATCH ANTENNA ARRAY.

Parameter	Single patch	$1 \times 2$ patch array	$2 \times 2$ patch array
$f_r$ GHz	28.018	28.017	27.979
$S_{11}$ dB	-39	-35	-32
3D directivity(dB)	7.68	10.6	12.7
BW (MHz)	550	457	700
E-Plane HPBW $\theta_E$	$72.6^\circ$	$36.2^\circ$	$36.2^\circ$
H-Plane HPBW $\theta_H$	$80.9^\circ$	$78^\circ$	$45^\circ$
Element spacing	----	$dy=0.6\lambda$	$dy=0.6128\lambda$ $dx=0.85\lambda$

E. Steering capability of the designed  $2 \times 2$  patch array

In order to determine the optimum steering capability of the designed  $2 \times 2$  planer array, a polar radiation patterns  $g_E(\theta, \phi)$ ,  $g_H(\theta, \phi)$  in E & H-planes of the array have been calculated by using (A.10), (A.13) [Appendix. A] for  $M=2, N=2$ , with optimum elements spacing  $dx = 0.85\lambda$ ,  $dy = 0.6128\lambda$  and a particular steering angles ( $0^\circ, 10^\circ, 15^\circ, 20^\circ, 25^\circ, 30^\circ, 35^\circ, 40^\circ$ ) respectively and plotted as in Fig. 11. In each case HPBW  $\theta_E, \theta_H$  in E&H planes, 3D-directivity by using (A.14), normalized side lobe magnitude in E & H planes, and loss in directivity are determined, and plotted as in Fig. 12.



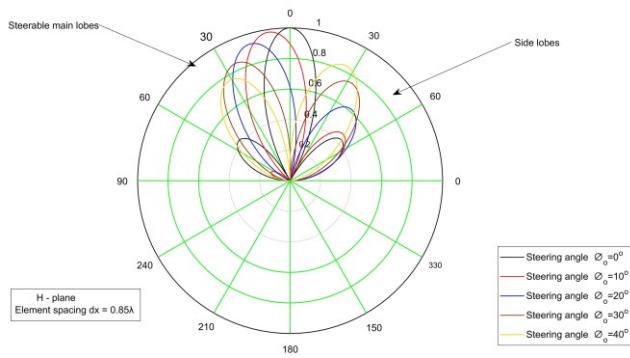
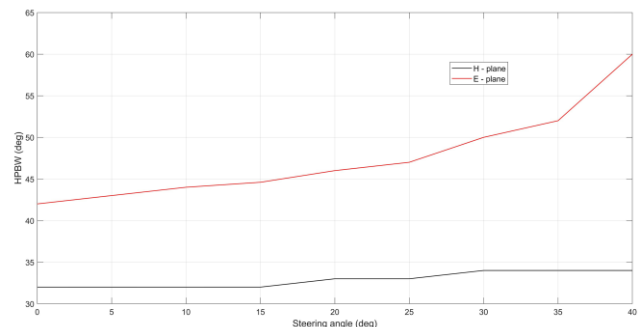
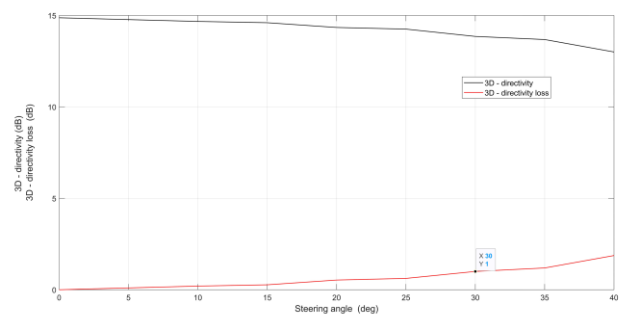


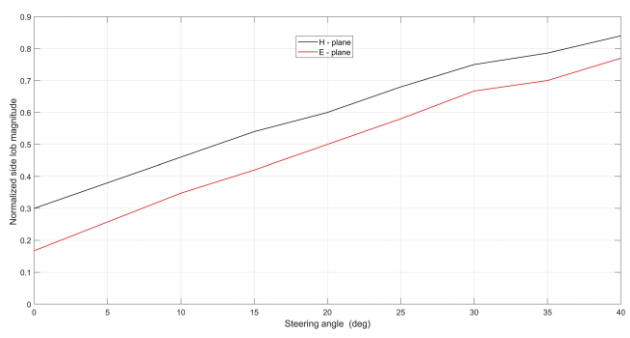
Fig 11. Radiation patterns of 2x2 circular patch antenna array for different steering angles (deg) (a) E-plane (b) H-plane



(a)



(b)



(c)

Fig. 12. Calculated performance for 2x2 circular patch antenna array as a function of steering angle (a) H-PBW in E & H planes, (b) 3D-directivity & directivity loss, (c) Normalized side lobe magnitude in E & H planes

Fig. 12 illustrate that as we steer from the broadside toward end fire, the following degradation in antenna response will be noticed as in the following:

1. The HPBW broadened as in Fig. 12(a) and (b), hence the 3D directivity decreases, and this will limit the steering capability up to  $(\pm 30^\circ)$  at which the directivity decreases to acceptable value (1dB loss below the directivity at  $0^\circ$ ) as shown in Fig. 12(b).

2. The side lobe magnitude grows as in Fig. 12(c), hence this degradation in antenna performance will increase the interference in mobile system,

This limitation in the steering capability up to  $(\pm 30^\circ)$  of the designed 2x2 circular patch antenna array is not enough to achieve a broad space coverage at mobile station therefore to overcome such limitation we propose to place four identical 2x2 arrays on the four edges of mobile station (MS) substrate as shown in Fig. 13.

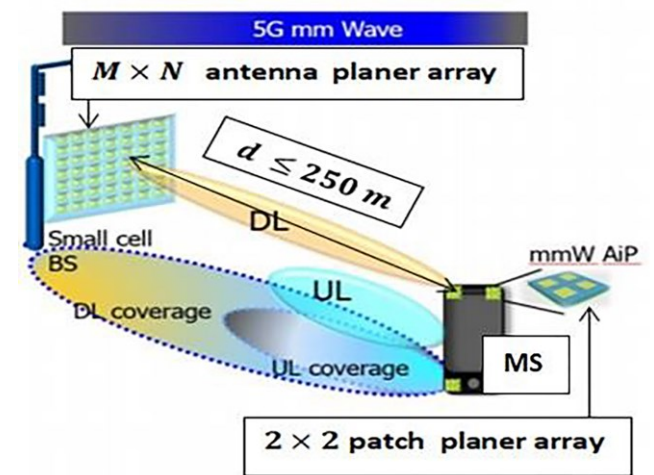


Fig. 13. 5G-mm mobile system micro-cell

CONCLUSION

This work presents optimized results for single element micro strip circular patch antenna, two elements 1x2 circular patch antenna array, and four element 2x2 circular patch antenna array which can be used in mm-5G mobile station. It is observed from the results that the narrower beamforming has been achieved as the number of patch elements increased. Also it is noticed that the return loss, 3D-gain, impedance bandwidth for the designed array are increased.

The spacing between the elements of the array play important role in antenna array performance, where as the separation between the element increases the side lobe grows which leads to increase the interference level in mobile system which is reflected to more system performance degradation.

Theoretical results shows that as we steer from the broadside to end fire the side lobe grows hence interference will increase as well as the 3D-gain decreases therefore their will be performance degradation which will limit the steering capability up to  $\pm 30^\circ$ .

To overcome the limitation in steering capability this work propose to place four identical 2x2 circular patch antenna arrays at different edges of mobile phone substrate to achieve broad space coverage by steering the beams of the mobile station arrays.

## REFERENCES

- [1] N. L. Vamsi Priya. K, G. Sai Sravanthi, K. Narmada, K. Naga Kavya, G. Yedukondalu Swamy, M. Durgarao "A Micro strip Patch Antenna Design at 28 GHz for 5G Mobile Phone Application," International Journal of Electronics, Electrical and Computational System, Vol. 7, no. 3, pp. 204-208, March 2018.
- [2] Z. hasan, A. Zaman, and A. Ahmed, "Design and Fabrication of a circular Micro strip Patch Antenna for GPS Application," *International Journal of Electronics & Communication Technology (IJEET)*, Vol. 8, no. 3, pp. 54-57, July – Sept 2017.
- [3] Abdulsattar. M. Ahmed, Salim. Abdulla. Hasan, Sayf. A. Majeed, "5G Mobile Systems, Challenges and Technologies: A Survey," *Journal of Theoretical and Applied Information Technology*, Vol. 97, no. 11, 15<sup>th</sup> June 2019. <https://doi.org/10.5281/zenodo.3256485>
- [4] Sridhar Rajagopal, Shadi Abu Surra, Zhouyue Pi and Farooq Khan. "Antenna Array Design for Multi Gbps mm Wave," *Mobile Broadband Communication. IEEE Globecom 2011 Proceeding* <https://doi.org/10.1109/GLOCOM.2011.6133699>
- [5] I. J. Bahland P. Bhartia, "Microwave Antenna," *Artech Trans, Propagation*. Vol. AP-30, No.4, PP. 645-650, July 1982.
- [6] C.A., Balanis, "Advanced Engineering Electromagnetic," John Wiley and son New York 1989.
- [7] K.R. and J Mink, "Micro Strip Antenna Technology," *IEEE Trans Propagat*, Vol. AP-29, No. 1, pp. 2-27, January 1981. <https://doi.org/10.1109/TAP.1981.1142523>
- [8] Z. Ying, "Antenna in Cellular Phones for Mobile," In *Proceeding of IEEE*. Vol. No. 100. Pp. 2286-2296, July 2012. <https://doi.org/10.1109/JPROC.2012.2186214>
- [9] C. A. Balains, "Antenna Theory Analysis and Design," 3<sup>rd</sup> Ed. John Wiley & Sons. New Jersey, 2005.
- [10] Vamsi Priya.K, "A Micro Strip Patch Antenna Design at 28 GHz for 5G Mobile Phone Application," *International journal of Electronic and Computational System*, Issn 2348-117X, Volume 7, Issue 3, March 2018.
- [11] Kirankumar A. Solanki, Gautam. D. Mokwana, "Study and Analysis of Micro Strip Patch Array at 12 GHz for 5G Application," *Journal of Remote Sensing GIS and Technology*, Volum 4 Page 1-8 Issue1, 2018.
- [12] Sonali Jain, Rajesh Nema, "Review Paper for Circular Micro Strip Patch Antenna," *International Journal of Computer Technology and Electronic Engineering*, Volume 1, Issue 3, issn 2249 6343.
- [13] Hamid Mubarak Mustafa, "Performance Evaluation of 1 × 2 Patch Antenna Array Based on Power Divider Characteristics," 2106 *Conference of Basic Science and Engineering Studies (SGCAC)*. <https://doi.org/10.1109/SGCAC.2016.7457998>
- [14] Rahman, Qunsheng Cao, Ishfaq Hussain, Hisham Khalil, Muhammad Zeeshan, and Wasseem Nazar, "Design of Rectangular Antenna Array for 5G Wireless Communication," *Progress In Electromagnetics Research Symposium Spring (PIERS)*, St Petersburg Russia, 22 – 25 May 2017. <https://doi.org/10.1109/PIERS.2017.8261995>
- [15] Qurratul Ayn, Nageswar Rao, Malikarjuna Rao, "Design and Analysis of High Gain 2 × 1 and 4 × 1 Circular Patch Antenna Arrays for 2.4 GHz Application," *International Journal of Innovative Research in Science Engineering and Tecnology*. Vol 6, Issue 8, August 2017.
- [16] Z.Ying, "Antenna in Cellular Phones for Mobile," In *Proceeding of IEEE*. Vol. No. 100. PP 2286-2296, July 2012 <https://doi.org/10.1109/JPROC.2012.2186214>
- [17] Md Ziaur Rahman, Mohammed Mynuddin, Kartik Chandra Debnath, "The significance of Notch Width on the performance of Inset Feed Rectangular Microstrip Patch Antenna," *International Journal of Electromagnetics amd Application* 2020, 10(1): 7-18 <https://doi.org/10.5923/ijea.20201001.0>
- [18] D. Prabhakar, Dr. P. Mallilarjuna Rao, DR. M. Satyanarayana, "Characteristic of Patch Antenna with Notch gap Variations for Wi-

Fi Application," *International Journal of Applied Engineering Research* ISSN 0973-4562 Volume 11, Number 8(2016) pp 5741-5746.

## APPENDIC A

## RADIATION PATTERN OF TWO DIMENSIONAL PLANER ANTENNA ARRAY

The configuration of the two dimensional  $M \times N$  antennas planer array in xy plane is shown as in Fig. A.1.

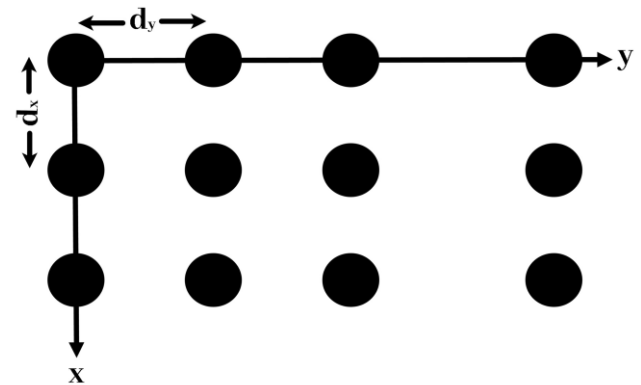


Fig. A.1.  $M \times N$  planer patch antenna array configuration in xy plane

The normalized array factor  $A(\theta, \phi)$  of  $M \times N$  dimensions planer array can be obtained from the following equation[1]

$$A(\theta, \phi) = \left[ \frac{\sin\left(\frac{M\psi_M}{2}\right)}{M\sin\left(\frac{\psi_M}{2}\right)} \right] \left[ \frac{\sin\left(\frac{N\psi_N}{2}\right)}{N\sin\left(\frac{\psi_N}{2}\right)} \right] \quad (\text{A.1})$$

$$\psi_N = kd_y \sin(\theta) \sin(\phi) + \beta_N \quad (\text{A.2})$$

$$\psi_M = kd_y \sin(\theta) \cos(\phi) + \beta_M \quad (\text{A.3})$$

$$\beta_M = kd_x \sin(\theta_o) \cos(\phi_o) \quad (\text{A.4})$$

$$\beta_N = kd_y \sin(\theta_o) \sin(\phi_o) \quad (\text{A.5})$$

Where,

$M$ : is the number of elements along  $x$  – direction

$N$ : is the number of elements along  $y$  – direction

$\psi_M$  and  $\psi_N$ : indicate the array phase along the  $x$  -and  $y$ -axis respectively

$\beta_M$  and  $\beta_N$ : denote the scanning steering factors along  $x$  and  $y$  in function of the steering angle

$\theta_o$ : is the steering elevation angle

$\phi_o$ : is the steering azimuth angle

$d_x$ : is the spacing between the elements placed along  $x$  direction

$d_y$ : is the spacing between the elements placed along  $y$  direction

$k$ : is phase constant and given by

$$k = \frac{2\pi}{\lambda} = \frac{2\pi f}{c} \quad (\text{A.6})$$

In general radiation pattern of array is given by

$$g(\theta, \phi) = A(\theta, \phi) F(\theta, \phi) \quad (\text{A.7})$$



Where,  $F(\theta, \phi)$  is the normalized radiation pattern of the single element

For single circular patch antenna the normalized radiation pattern in E – plane is given by [1]

$$F_E(\theta, \phi = 0^\circ) = j'_{02} \quad (\text{A.8})$$

Where,

$$j'_{02} = j_o(ka_e \sin\theta) - j_2(ka_e \sin\theta) \quad (\text{A.9})$$

To determine the normalized radiation pattern for  $M \times N$  antenna array in E – plane substitute for  $F_E(\theta, \phi = 0^\circ)$  from (A.8) into (A.7) then

$$g_E(\theta, \phi) = j'_{02} \left[ \frac{\sin\left(\frac{M\psi_M}{2}\right)}{M \sin\left(\frac{\psi_M}{2}\right)} \right] \left[ \frac{\sin\left(\frac{N\psi_N}{2}\right)}{N \sin\left(\frac{\psi_N}{2}\right)} \right] \quad (\text{A.10})$$

For single circular patch antenna the normalized radiation pattern in H – plane is given by [1]

$$F_H(\theta, \phi = 90^\circ) = j_{02} \cos(\theta) \quad (\text{A.11})$$

Where,

$$j_{02} = j_o(ka_e \sin\theta) + j_2(ka_e \sin\theta) \quad (\text{A.12})$$

To determine then normalized radiation pattern for  $M \times N$  antenna array in H – plane substitute for  $F_H(\theta, \phi = 90^\circ)$  from (A.11) into (A.7) then

$$g_H(\theta, \phi) = j_{02} \cos(\theta) \left[ \frac{\sin\left(\frac{M\psi_M}{2}\right)}{M \sin\left(\frac{\psi_M}{2}\right)} \right] \left[ \frac{\sin\left(\frac{N\psi_N}{2}\right)}{N \sin\left(\frac{\psi_N}{2}\right)} \right] \quad (\text{A.13})$$

The 3D directivity  $D_o$  (maximum directive gain) of patch is given by [9]

$$D_o = \frac{30000}{\theta_E \theta_H} \quad (\text{A.14})$$

Where  $\theta_E$  (deg): the HPBW in E-plane, and  $\theta_H$  (deg): the HPBW in H-plane.